Progress In Electromagnetics Research M, Vol. 70, 11–20, 2018

Triple-Band Printed Dipole Antenna for RFID/GPS/BLE Applications

Khodor Jebbawi*, Matthieu Egels, and Philippe Pannier

Abstract—Progress in wireless communication requires antennas that work on multi-band simultaneously. This paper presents a design method for a multi-band antenna using printed dipole with L-slots fed by a single coaxial cable. Using this method, a triple-band antenna that operates at 868–915 MHz for RFID (radio frequency identification), 1575 MHz for GPS (global positioning system) and 2.45 GHz for BLE (bluetooth low energy) was designed and manufactured. The antenna's parameters for triple-band operation are investigated and discussed. In this antenna design, ANSYS HFSS software using highly accurate finite element method (FEM) simulation is employed to analyze the entire structure. The designed antenna is manufactured using an FR-4 substrate with a dielectric constant (ϵ_r) of 4.4 and thickness (h) of 1.6 mm. Many prototypes have been fabricated, and good agreement between simulations and measurements has been achieved. The performance of the prototypes has been measured in a standard far-field anechoic chamber. The proposed triple-band antenna is also tested by measuring the reading distance, and it is found that the proposed antenna can be used for RFID applications.

1. INTRODUCTION

Multi-standards antennas have received significant importance due to the limited room in modern portable wireless communication devices which may require an antenna to work at several frequencies simultaneously. This antenna should be planar, lightweight, and compact, so that it can be easily embedded in active devices for wireless communications. Therefore, there are various multi-band antennas that have been developed over the years, which can be utilized to achieve multi-band operations, such as PIFA [1], monopole antenna [2] and others [3, 4], while printed dipole antennas are attractive because they are simple, easy to fabricate and easy to interface with an Application Specific Integrated Circuit (ASIC) microchip [5]. In recent years, several multi-band printed dipole antennas have been reported. A triple-band printed dipole antenna using parasitic elements was proposed in [6]. In [7], a triple-band omnidirectional antenna which comprises three pairs of dipoles placed back to back and printed on a dielectric substrate was presented for WLAN applications (2.4 GHz, 5.2 GHz and 5.8 GHz). A coplanar dipole antenna with an inverted-H slot has already been proposed for 0.9/1.575/2.0/2.4/2.45/5.0 GHz applications [8]. Most of these designs use an electromagnetic simulation software (HFSS, CST, FEKO) to analyse the entire structure. [12–14] present designs with microstrips, flanges, strips and patches. The added value of these papers is that they refer to semi-analytical methods for treating the devices and structures.

A systematic method for designing a multi-band antenna is an approach that can be applied to any set of target frequencies. Existing techniques such as [5] of designing multi-band printed dipole antenna are not fully systematic, since they do not allow to control and manage all bands. [5] presents

Received 2 May 2018, Accepted 9 June 2018, Scheduled 22 June 2018

* Corresponding author: Khodor Jebbawi (Khodor.jebbawi@im2np.fr).

The authors are with Institut Materiaux Microelectronique Nanosciences de Provence, UMR CNRS 7334, Aix-Marseille Universite, 5 rue Enrico Fermi, Batiment Neel, Technopole de Chateau Gombert, 13453 Marseille Cedex 13, France.

an antenna that operates at three different frequencies by connecting two branches to the prime dipole. However, the goal of that study was not to define a systematic methodology for designing multi-band antennas but to design a specific multi-band antenna for RFID. The multi-band antenna designed in this work is a typical application of the new proposed design methodology. In [6], a triple-band operation is achieved by using a dipole with parasitic elements. This design is printed on two metallic layers which makes it more complex. Moreover, the parasitic element is fed by coupling from the driving dipole which reduces the performances, especially the gain of the band provided by the parasitic element.

This work proposes a systematic method to achieve a multi-band antenna using a dipole with L-slots fed through a single feeding port. This method provides a formula in order to compute the length of the L-slot for any target frequency. In addition, the management and control of the resonant frequency for each band without affecting the other bands is available by changing the length of the L-slot responsible for that band. This proposed method is applied in order to design a triple-band printed dipole antenna for RFID (868–915 MHz), GPS (1575 MHz) and BLE (2.45 GHz). The triple-band antenna is printed on a single metallic layer and presents a very good return loss, bandwidth and gain for each band.

A typical application for this type of antenna can be the monitoring of patients and the tracking of logistics for a large multi-side medical institute. In each of the branches, a network of mobile readers are implanted, each of which embedded with the proposed antenna. The RFID band is used for reading the data (temperature, pulse) stored in UHF RFID tag placed on the arms of patients. The BLE band is meant for sending the information to the data center. The relatively exact position of each reader can be provided by GPS band.

In order to validate the performance of the fabricated antenna, a functional RFID reading distance test is applied on the first band (UHF RFID) of the proposed antenna by using a commercial Reader module (Micro ThingMagic [9]) and commercial tag (Lintrak C [10]).

2. ANTENNA DESIGN

This section presents the followed methodology to design a multi-band dipole antenna with L-slots. The proposed approach begins with single resonant frequency. Start with the simple dipole in Figure 1(a) to show the steps of this methodology. This dipole has a single resonant frequency at 868 MHz (L is about $\lambda_0/2$ in free space) as shown in Figure 2(a). Figure 2(b) presents the imaginary component of the impedance $\mathrm{Im}(Z_{11})$ against frequency. It is observed that a mode resonates when the value of $\mathrm{Im}(Z_{11})$ changes sign, while increasing. This phenomenon is known as inductive resonance.

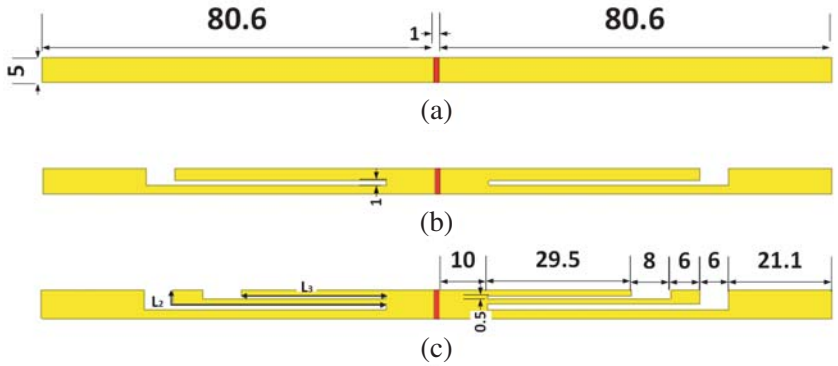

Figure 1. Geometry of the simple dipole (a) without slots, (b) with one L-slot, (c) with two L-slots (units: mm).

After the resonant frequency has been achieved exactly at the center of the first desired band, L-shaped slots were inserted in the dipole to achieve multiband operation. These slots were inserted one by one inside the dipole, where the length of each slot is about $\lambda/2$ of the target frequency. Figure 1(b) shows the dipole with one L-slot ($L2$) for double-band operation. Figure 1(c) shows the dipole with two L-slots ($L2, L3$) for triple-band operation. Each L-slot adds a new band as shown in Figure 3(a). The

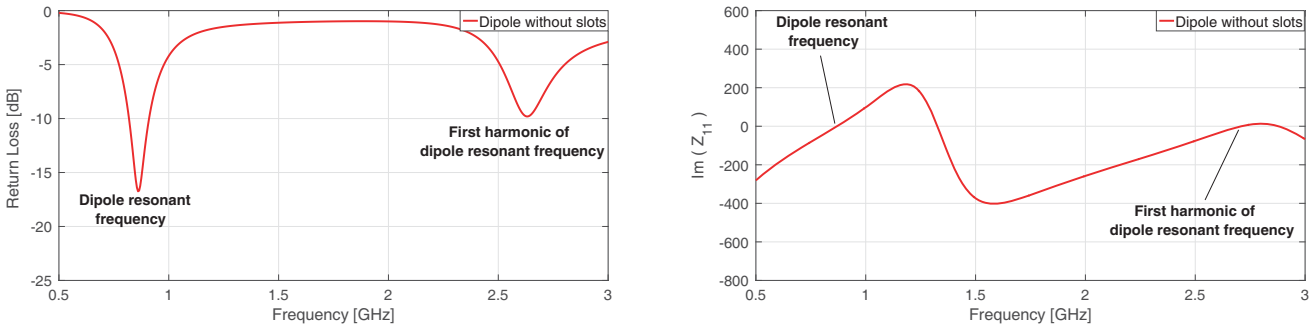

Figure 2. (a) S_{11}, (b) $\mathrm{Im}(Z_{11})$ of the dipole shown in Figure 1(a).

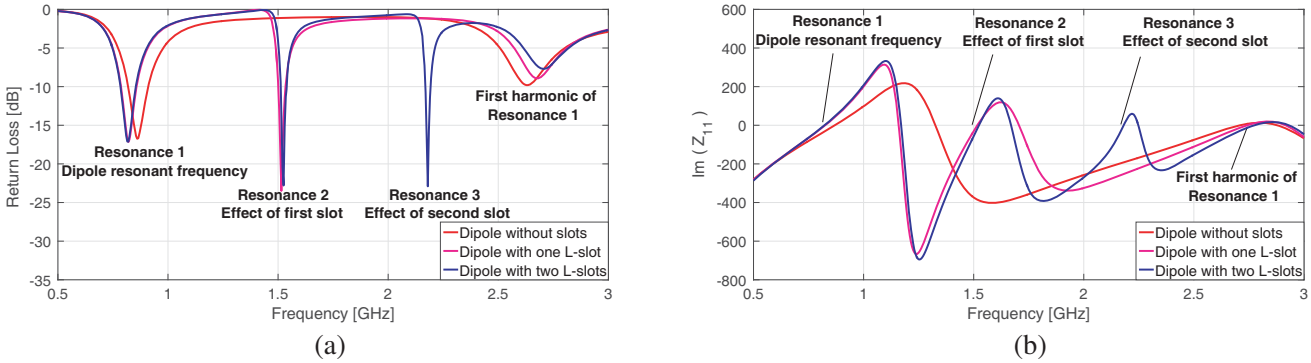

Figure 3. (a) S_{11}, (b) $\mathrm{Im}(Z_{11})$ of the different dipoles shown in Figure 1.

L-shaped slot creates a new branch element which modifies the profile of the $\mathrm{Im}(Z_{11})$ by increasing the number of inductive resonances at high frequencies as shown in Figure 3(b).

The approach mentioned above is used to design a triple-band antenna for RFID (868–915 MHz), GPS (1575 MHz) and BLE (2.45 GHz). The length of the dipole is the only parameter that affects the resonant frequency of the first band. On the other hand, the parameters that affect the higher resonant frequencies of the antenna are the L-slots lengths. As the antenna is a symmetrical dipole, the length of each of these branches $L1$, $L2$ and $L3$ is about a quarter of the effective wavelength of the target frequency. Moreover, the dipole used is a slot line of rectangular geometry, so the formula in [11] of slot transmission line can be used to calculate the value of ϵ_{eff}, λ_{eff} and L_{eff} as follows.

The effective dielectric constant (ϵ_{eff}) of a slot line:

$$\epsilon_{eff} = \frac{(\epsilon_r + 1)}{2} \tag{1}$$

The effective length of each branch of dipole:

$$L_{eff} = \frac{\lambda_{eff}}{4} = \frac{c}{\left(\sqrt{\epsilon_{eff}} \times f \times 4\right)} \tag{2}$$

where

λ_{eff} = Effective wavelength

c = Velocity of light

f = Target frequency

ϵ_r = Dieletric Constant

The geometry and photograph of the proposed antenna are presented in Figure 4. The optimal geometrical parameters of the proposed antenna are obtained by using Ansoft high-frequency structure

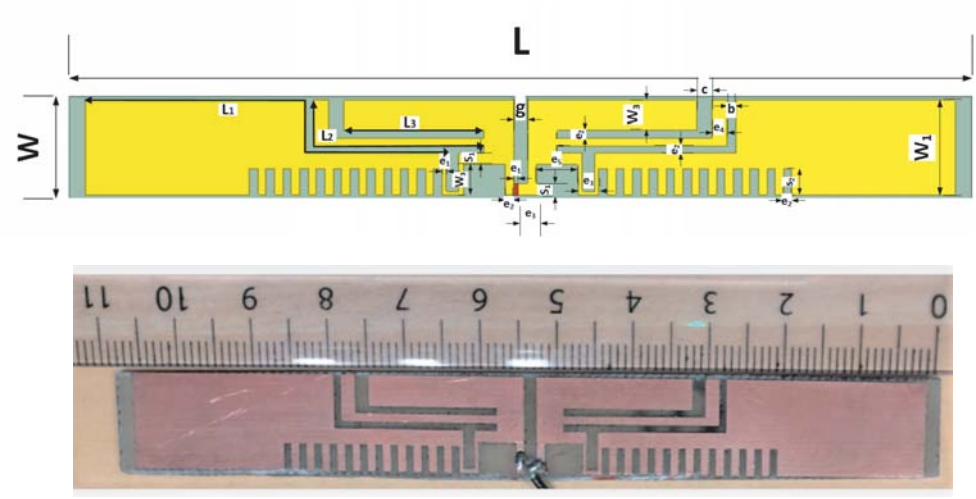

Figure 4. Geometry and photograph of the proposed antenna.

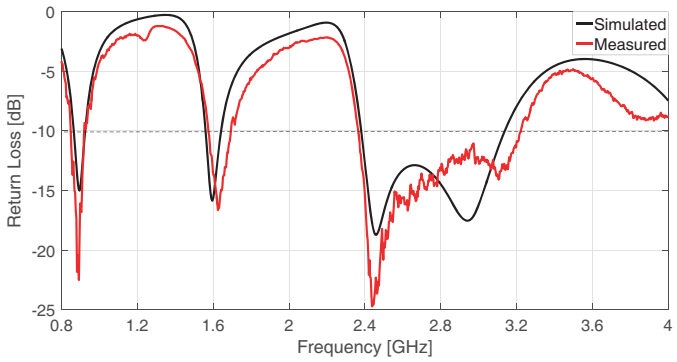

Figure 5. Simulated and measured S_{11} of the proposed antenna.

Table 1. Parameters of the proposed antenna (units: mm).

L	L_1	L_2	L_3	e_1	e_2	e_3	e_4	e_5	S_1	S_2	W	W_1	W_3	g	b	c
107.7	50	26.3	16.7	0.5	1	2.5	1.8	5	1.5	3.5	13.5	12.5	4	1.7	1	1.8

simulator version 17. The discrete port of 50 Ω was placed across a 0.5 mm gap at the center of the antenna. As shown in Figure 4, the triple-band antenna is designed and printed on a single metallic layer 107.7 × 13.5 mm^2 of an FR4 dielectric substrate which has permittivity of 4.4 and thickness of 1.6 mm. All detailed parameters of the proposed antenna are summarized in Table 1.

The dipole which has a resonance frequency at 900 MHz is altered by two L-shaped slots, $L2$ and $L3$, which add two additional bands at 1575 MHz and 2.45 GHz, respectively. Small rectangular slots were placed on the dipole in order to reduce the size of the proposed antenna. The aim of these rectangular slots is to shift the first resonant frequency to lower frequencies without adding inductive resonances. The measurement of return loss is done using a Rohde & Schwarz ZVA24 Network Analyzer. Figure 5 shows simulated and measured return losses (S_{11}) of the proposed antenna as a function of frequency. The measured results are in good agreement with the predicted simulated ones. Results obtained indicate that the proposed antenna provides triple operating frequencies of 900 MHz, 1575 MHz and 2.45 GHz and three good bandwidths ($S_{11} < -10$ dB) of 61 MHz (at 900 MHz), 83 MHz (at 1575 MHz) and 758 MHz (broadband at 2.45 GHz).

The broadband at the third resonant frequency (2.45 GHz) is due to the coupling between the first harmonic of the first resonant mode and the third resonant frequency. This is achieved by decreasing b and keeping e_4 fixed. The effect of b on the bandwidth of 2.45 GHz is shown in Figure 6(a) which depicts the return loss of the proposed antenna against frequency with different values of b. It is observable that the bandwidth at 2.45 GHz increases when the value of b decreases, while e_4 remains fixed. Moreover, the coupling between $L1$ and $L3$ can be found in Figure 6(b) by plotting the surface current distributions of the proposed antenna at 2.45 GHz.

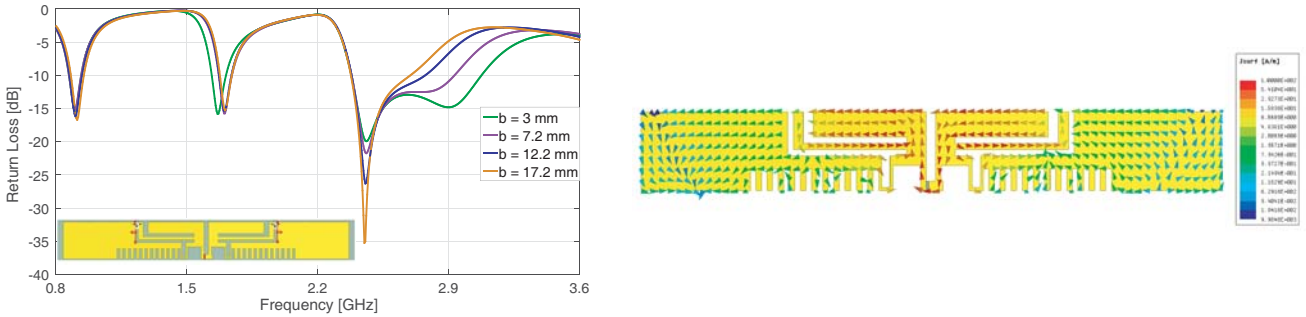

(a) (b)

Figure 6. (a) S_{11} of the proposed antenna with different values of b. (b) Simulated surface current distributions of the proposed antenna at 2.45 GHz.

3. RESULTS AND DISCUSSION

A study on the effects of parameters $L2$ and $L3$ on the impedance matching for the proposed antenna is conducted, while $L1$ remains fixed at 50 mm. Figure 7(a) and Figure 8(a) respectively show the simulated return loss and realised gain with respect to the variation of $L3$. In this case, $L2$ is fixed at 26.3 mm, and as we can see in Figure 7(a) and Figure 8(a), the third resonant frequency is shifted to lower frequencies and decoupled from the harmonic of first resonant frequency when the length of $L3$-slot increases, while keeping c fixed. Setting $L3$ to 16.7 mm, the effect of the variation of $L2$ can be shown in Figure 7(b) and Figure 8(b) which indicate that the GPS band undergoes the same shift effect as the 2.45 GHz band when the length of $L2$-slot increases, while keeping b fixed. Therefore, the only parameter that affects the resonance frequency of any band is the length of the dipole or L-slot which provides that particular band.

Graphs of measured and simulated gains versus frequency of the proposed antenna are plotted in Figure 9. It is observed that the antenna has a good gain in the operating bands and a very small gain

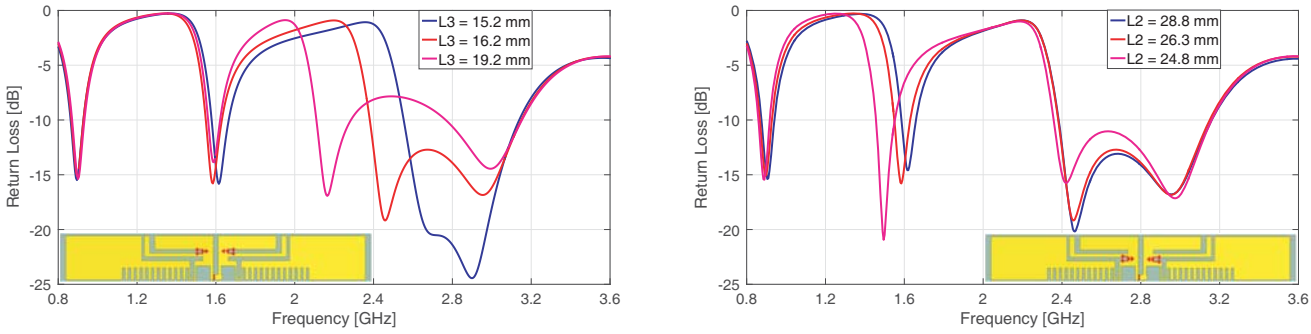

(a) (b)

Figure 7. S_{11} of the proposed antenna as the function of frequency for different values of (a) $L3$, (b) $L2$.

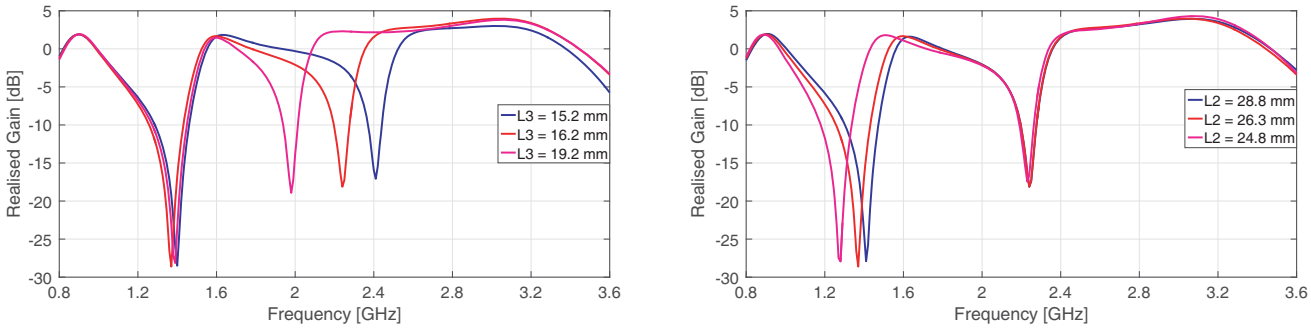

Figure 8. Realised gain of the proposed antenna as the function of frequency for different values of (a) $L3$, (b) $L2$.

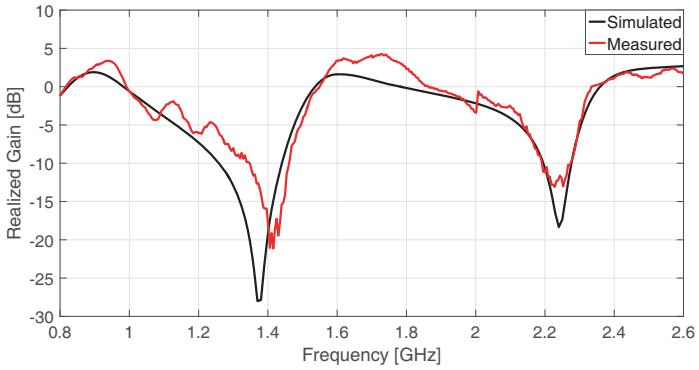

Figure 9. Simulated and measured gain of the proposed antenna.

Table 2. Simulated and measured results of triple-band printed dipole antenna.

	Frequency (GHz)					
	0.9		1.575		2.45	
	Simulated	Measured	Simulated	Measured	Simulated	Measured
Return Loss (dB)	−15	−16.6	−13	−10.1	−19	−23.7
Bandwidth (MHz)	61	70	83	115	758	852
Gain (dB)	1.91	2.6	1.38	1.98	2.13	1.75

outside those bands. Figure 10 shows the measured and simulated gains for each band. Table 2 shows the simulated and measured results of the proposed triple-band antenna in term of input return loss, bandwidth and gain. The measured bandwidth is recorded for $S_{11} < -10$ dB. The differences between the simulated and measured gains of the antenna are 0.7 dB, 0.6 dB and 0.38 dB at 900 MHz, 1575 MHz and 2.45 GHz, respectively.

The radiation patterns of the fabricated antenna are measured in an anechoic chamber. The measured E-plane and H-plane radiation patterns at 868 MHz, 900 MHz, 920 MHz, 1575 MHz and 2.45 GHz are presented in Figure 11. The patterns exhibit 8-shaped omnidirectional patterns for E-plane. Circular radiation patterns are observed for H-plane for the proposed antenna.

Table 3 shows a comparison between the proposed antenna and coplanar dipole antenna with Inverted-H Slot [8] which operates at same frequencies and etched on the same type of substrate as the proposed antenna. This comparison is in terms of antenna size, total area occupied by the antenna and measured peak gains (E-Plane and H-Plane) at 900 MHz, 1575 MHz and 2.45 GHz. From this table, it

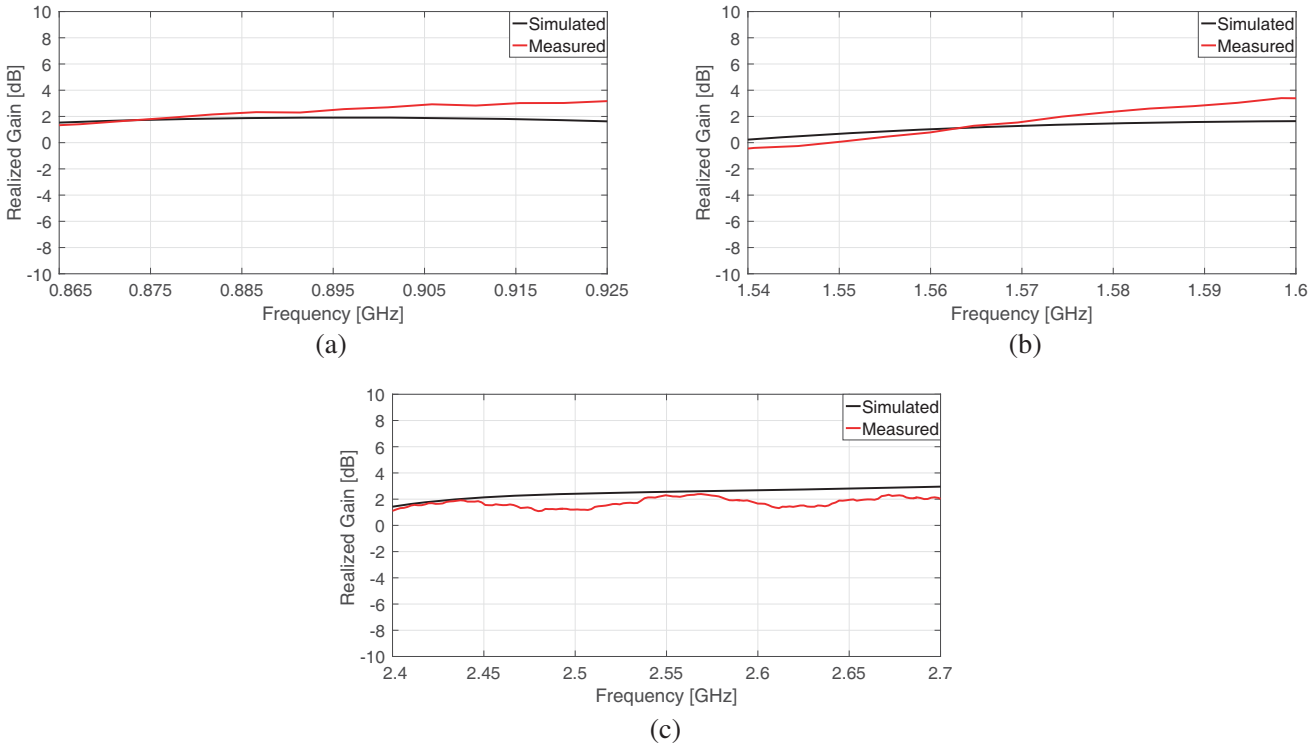

Figure 10. Simulated and measured gain for each band, (a) RFID band, (b) GPS band, (c) BLE band.

Table 3. Comparison of the proposed antenna performance with [8].

Antenna	Size (mm^2)	Total area occupied (mm^2)	Peak Gain (dB)					
			900 MHz		1575 MHz		2.45 GHz	
			E-Plane	*H*-Plane	*E*-Plane	*H*-Plane	*E*-Plane	*H*-Plane
Published literature [8]	123×31	3813	3.11	2.18	1.25	1.05	3.17	1.26
Proposed antenna	107.7×13.5	1454	3.59	3.05	3.72	1.65	2.3	2.62

Table 4. Reading distance of proposed antenna in vertical/horizontal orientation at 868 MHz.

	Reading distance (cm)	
Power (dBm)	Vertical	Horizontal
5	17	20
10	30	33
15	52	52
20	130	135

can be seen that the proposed antenna is the smallest and has the highest *E*-Plane/*H*-Plane gains for all bands. The majority of the reported multi-band antennas have the drawbacks of large size and/or limited frequency of operation compared with the proposed design in this paper. This antenna also has a simple structure with ability of management and tunability of bands which other designs rarely offer.

Then, as shown in Figure 12 the fabricated antenna is connected to a UHF RFID reader module (Micro from ThingMagic) in order to measure the reading distance at different values of power using a

commercial UHF RFID tag (Lintrak C). The measurement is taken in vertical and horizontal orientations for (tag, proposed antenna). As shown in Table 4, the proposed antenna has good reading distance values. Hence, it indicates that the proposed antenna can be used for UHF RFID system. Like the first band, the two other bands will be tested with commercial solution.

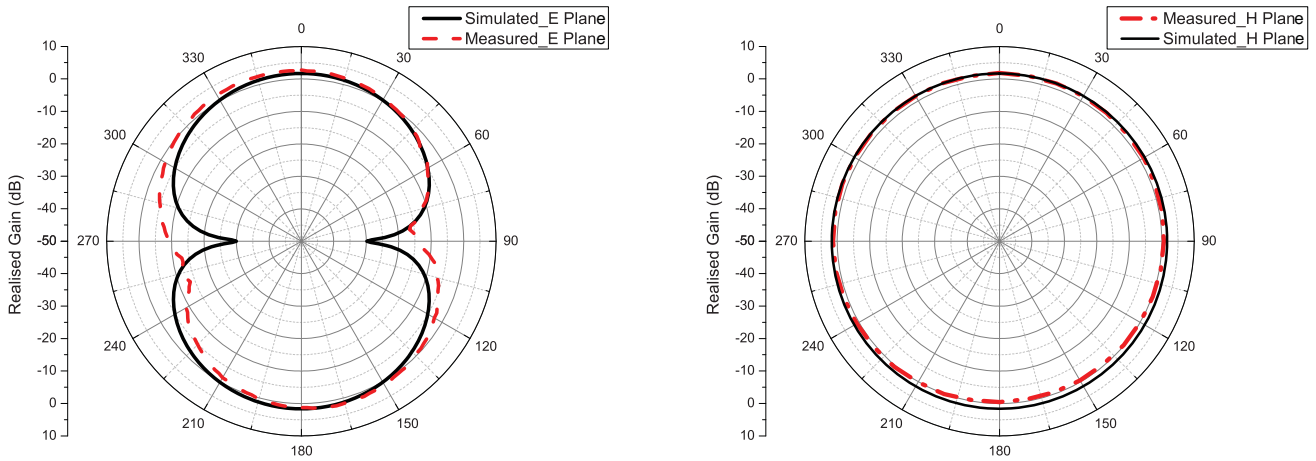

(a)

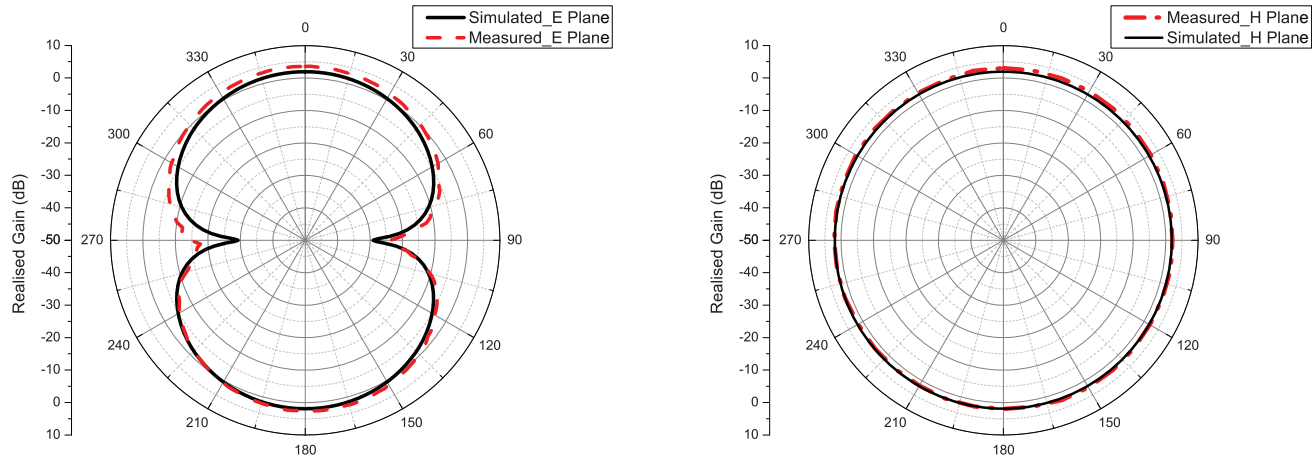

(b)

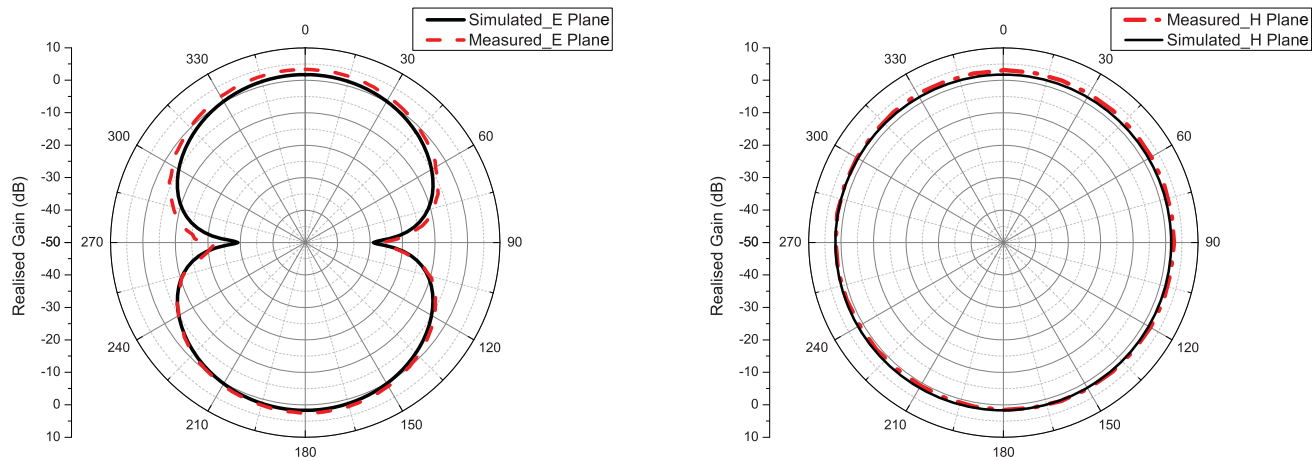

(c)

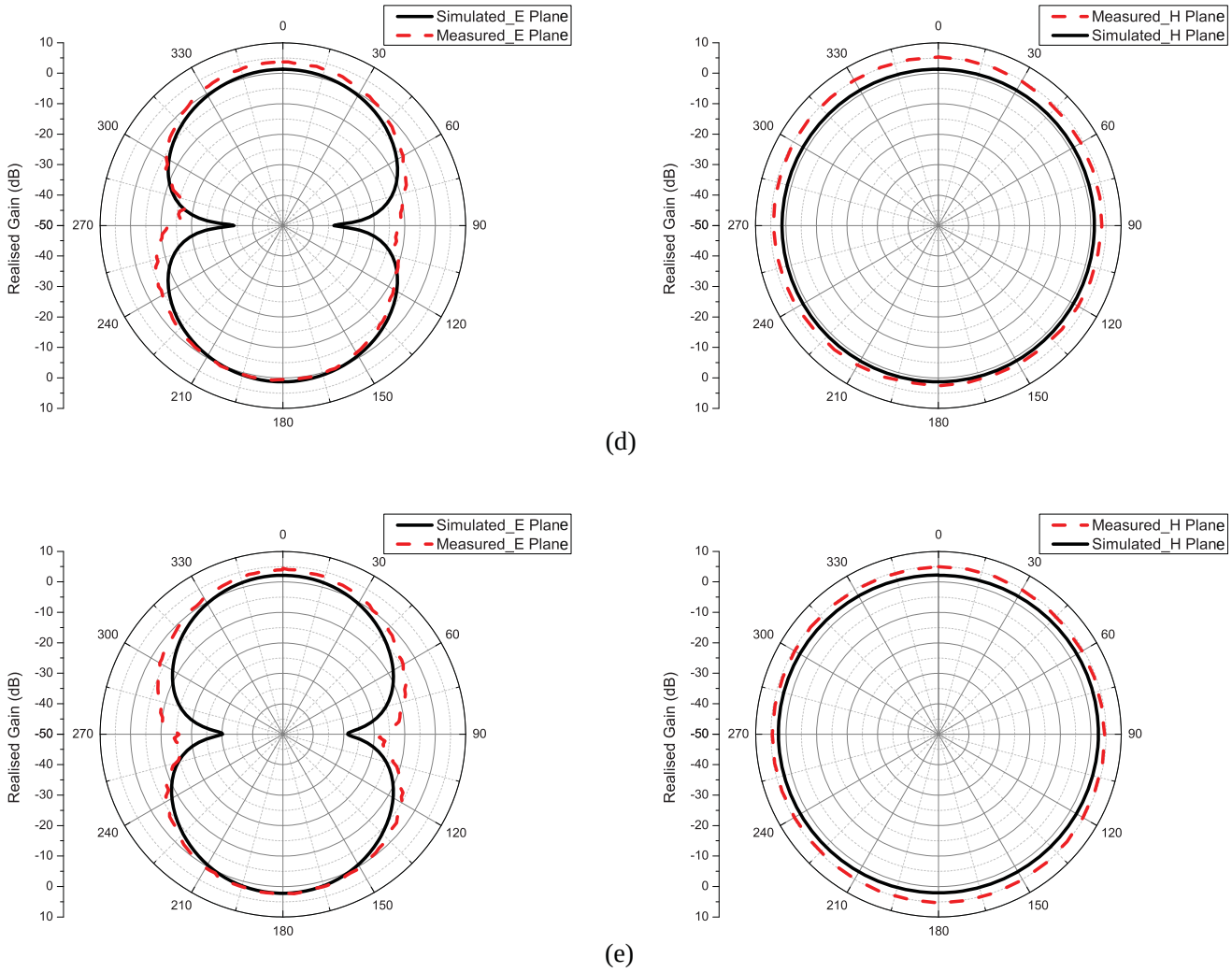

Figure 11. Simulated and measured radiation pattern of triple-band printed dipole antenna at (a) 868 MHz, (b) 900 MHz, (c) 920 MHz, (d) 1575 MHz, (e) 2.45 GHz.

Figure 12. Photography of RFID functional reading distance test of the proposed antenna in (a) vertical, (b) horizontal orientation.

4. CONCLUSION

In this paper, a design method for a multi-band antenna using dipole with L-shaped slots is presented. This method was applied to design a compact triple-band printed dipole antenna that operates at 868–915 MHz/1575 MHz/2.45 GHz for tracking and monitoring system. Prototypes of the proposed antenna were fabricated and tested. A very good return loss, bandwidth and gain have been achieved for each band of the proposed antenna.

REFERENCES

1. Elsadek, H. and D. M. Nashaat, "Quad band compact size trapezoidal PIFA antenna," *Journal of Electromagnetic Waves and Applications*, Vol. 21, No. 7, 865–876, 2007.
2. Pan, B., R. L. Li, J. Papapolymerou, J. Laskar, and M. M. Tentzeris, "Low-profile broadband and dual-frequency two-strip planar monopole antennas," *IEEE Antennas and Propagation Society International Symposium*, 2665–2668, 2006.
3. Deepu, V., K. R. Rohith, J. Manoj, M. N. Suma, K. Vasudevan, C. K. Aanandan, and P. Mohanan, "Compact uniplanar antenna for WLAN applications," *IEEE Electronic Letters*, Vol 43, 70–72, 2007.
4. Elrazzak, M. M. and M. F. Alsharekh, "A compact wideband stacked antenna for the tri-band GPS applications," *Active and Passive Electronic Components, Hindawi Publishing Corporation*, 2008.
5. Abu, M. and M. K. Abd Rahim, "Triple-band printed dipole antenna for RFID," *Progress In Electromagnetics Research C*, Vol 9, 145–153, 2009.
6. Chang, K., H. Kim, K. S. Hwang, I. J. Yoon, and Y. J. Yoon, "A triple-band printed dipole antenna using parasitic elements," *Microwave and Optical Technology Letters*, Vol 47, 221–223, 2005.
7. Wu, Y.-J., B.-H. Sun, J.-F. Li, and Q.-Z. Liu, "Triple-band omni-directional antenna for WLAN application," *Progress In Electromagnetics Research*, Vol 76, 477–484, 2007.
8. Lu, Y.-Y. and E. Lin, "Design of coplanar dipole antenna with inverted-H slot for 0.9/1.575/2.0/2.4/2.45/5.0 GHz applications," *Journal of Electrical and Electronic Engineering*, Vol 5, No. 2, 2017.
9. ThingMagic, http://www.thingmagic.com/index.php/embedded-rfid-readers/micro.
10. Invengo-Textile, https://www.invengo-textile.com/uhf-laundry-tags-and-hardware/lintrak/.
11. RFwireless-world, http://www.rfwireless-world.com/Articles/Slotline-basics-and-slotline-types.html.
12. Valagiannopoulos, C. A., "Electromagnetic propagation into parallel-plate waveguide in the presence of a Skew metallic surface," *Electromagnetics*, Vol 31, 593–605, Oct. 2011.
13. Valagiannopoulos, C., "On smoothening the singular field developed in the vicinity of metallic edges," *IJAEM*, 2009.
14. Bowen, P. T., A. Baron, and D. R. Smith, "Theory of patch-antenna metamaterial perfect absorbers," *PRA*, 2016.